Gas flow observer for a Scania Diesel Engine with VGT and EGR

Master's thesis
performed in **Vehicular Systems**

by
Andreas Jerhammar and Erik Höckerdal

Reg nr: LiTH-ISY-EX -- 06/3807 -- SE

February 10, 2006

Gas flow observer for a Scania Diesel Engine with VGT and EGR

Master's thesis

performed in **Vehicular Systems**,
Dept. of Electrical Engineering
at **Linköpings universitet**

by **Andreas Jerhammar and Erik Höckerdal**

Reg nr: LiTH-ISY-EX -- 06/3807 -- SE

Supervisor: **Jesper Ritzén, M.Sc.**
Scania CV AB
Johan Wahlström, Lic.
Linköpings Universitet

Examiner: **Assistant Professor Erik Frisk**
Linköpings Universitet

Linköping, February 10, 2006

	Avdelning, Institution Division, Department	**Datum** Date
	Vehicular Systems, Dept. of Electrical Engineering 581 83 Linköping	February 10, 2006

Titel Title	Gasflödesobservatör för en Scania Dieselmotor med VGT och EGR Gas flow observer for a Scania Diesel Engine with VGT and EGR
Författare Author	Andreas Jerhammar and Erik Höckerdal

Sammanfattning
Abstract

Today's diesel engines are complex with systems like VGT and EGR to be able to fulfil the stricter emission legislations and the demands on the fuel consumption. Controlling a system like this demands a sophisticated control system. Furthermore, the authorities demand on self diagnosis requires an equal sophisticated diagnosis system. These systems require good knowledge about the signals present in the system and how they affect each other.

One way to achieve this is to have a good model of the system and based on this calculate an observer. The observer is then used to estimate signals used for control and diagnosis. Advantages with an observer instead of using just sensors are that the sensor signals often are noisy and need to be filtered before they can be used. This causes time delay which further complicates the control and diagnosis systems. Other advantages are that sensors are expensive and that some engine quantities are hard to measure.

In this Master's thesis a model of a Scania diesel engine is developed and an observer is calculated. Due to the non-linearities in the model the observer is based on a constant gain extended Kalman filter.

Nyckelord Keywords	Diesel engine, EGR, VGT, Modelling, Linearization, Observer, Constant gain extended Kalman filter

Abstract

Today's diesel engines are complex with systems like VGT and EGR to be able to fulfil the stricter emission legislations and the demands on the fuel consumption. Controlling a system like this demands a sophisticated control system. Furthermore, the authorities demand on self diagnosis requires an equal sophisticated diagnosis system. These systems require good knowledge about the signals present in the system and how they affect each other.

One way to achieve this is to have a good model of the system and based on this calculate an observer. The observer is then used to estimate signals used for control and diagnosis. Advantages with an observer instead of using just sensors are that the sensor signals often are noisy and need to be filtered before they can be used. This causes time delay which further complicates the control and diagnosis systems. Other advantages are that sensors are expensive and that some engine quantities are hard to measure.

In this Master's thesis a model of a Scania diesel engine is developed and an observer is calculated. Due to the non-linearities in the model the observer is based on a constant gain extended Kalman filter.

Keywords: Diesel engine, EGR, VGT, Modelling, Linearization, Observer, Constant gain extended Kalman filter

Preface

This Master's thesis has been performed for Scania CV AB at the division of Powertrain Control System Development - Engine Software (NEE) during the autumn of 2005 and continues the work done by Swartling [Swa05] and others.

Thesis outline

Chapter 1 gives an introduction to the existing work and the objectives of this thesis.

Chapter 2 gives a short introduction in the theory of signal processing and describes the nature of the noise in the air mass flow sensor.

Chapter 3 introduces the existing model and the extended model.

Chapter 4 describes the observer design and the linearization of the model.

Chapter 5 explains the measurement setup.

Chapter 6 estimates and evaluates the parameters.

Chapter 7 presents the results achieved.

Chapter 8 discusses the conclusion and the future work.

Acknowledgment

Andreas Jerhammar and Erik Höckerdal
Södertälje, January 2006

Contents

Chapter 1

Introduction

The purpose of this thesis is to further improve the, at Scania, existing model and gas flow observer of a six cylinder Scania diesel engine with EGR and VGT. A concrete list of what this thesis will deal with is presented in Section 1.2 and the existing work regarding the model is presented in Section 1.1.1.

Those not familiar with the terminology in thermodynamics, engine modelling, observer design and acronyms in the automotive business should consult the notation section at the end of this thesis.

1.1 Background

Emission legislation on heavy trucks is getting stricter. To keep the emissions at a low level and to be able to detect when the emissions exceed the legislated levels, accurate models used for diagnostics and control have to be implemented. This is especially important for engines with VGT and EGR due to the extra degrees of freedom that these extra control signals result in.

1.1.1 Existing work

At Scania CV AB the work to create a mean value engine model (MVEM) started with a Master's thesis by Elfvik in [Elf02]. The physical model created was then simplified by Ritzén in [Rit03] to enhance the real time performance. Flärdh and Gustavsson extended the model in [OF03] with turbo compound and Ericson improved the EGR model in [Eri04]. Swartling introduced a gas flow observer in [Swa05] to be able to use feedback from different measured quantities which greatly improved the connection between the model and the reality.

1.2   Objectives

The objectives of this thesis are to:

- Describe the nature of the noise in the air mass flow sensor and, if it proves to be possible, integrate this signal in the model and the observer.

- Extend the existing mean value engine model with a model of the temperature in the intake manifold and add it as feedback to the observer.

- Extend the existing EGR system model with temperature and pressure states.

- Evaluate the observer with data from a Scania diesel truck.

- Linearize the non-linear engine model and examine how well the linearized model corresponds to the non-linear model.

- Examine the number of Kalman filters needed to get as good observer performance as possible.

- Examine if a more complex model gives a better observer or if it is better to keep the model complexity at a low level to ensure good real-time performance.

1.3   Target group

This work is first and foremost intended for employees at Scania CV and M.Sc. /B.Sc. students with basic knowledge in signal processing, control theory, vehicular systems and thermodynamics.

Chapter 2

Noise in the air mass flow sensor

To compensate for model errors an observer can used. The observer uses measured signals to estimate the states. Kalman theory requires knowledge about process noise and measurement noise. While examining the data describing the measurement noise [Swa05] proposed that more work has to be done regarding the description of the noise in the air mass flow sensor.

2.1 Sensor errors

The noise model in this thesis takes the following sensor errors into account:

- Bias

- Noise

Other errors exist, but they are small and are therefore often neglected. This is also the case in this thesis. A common way to model sensor errors is to use white Gaussian noise. Another approach is to use a stationary Gaussian process with an exponential auto correlation, a so called Gauss-Markov process. In this thesis the noise is modelled using white Gaussian noise. This choice is made for simplicity.

2.2 Variations in noise intensity

In [Swa05] a relation was found between the noise intensity in the sensors measuring p_{im}, p_{em} and n_{trb}, and the speed of the turbine. A second degree polynomial was proposed for the noise intensity,

$$I = a_0 + a_1 \cdot n_{trb} + a_2 \cdot n_{trb}^2, \tag{2.1}$$

and estimated $a_i, i = 1, 2, 3$ using data from an ETC-cycle. An ETC-cycle (European Transient Cycle) does not contain many stationary working points. Because of this it is hard to examine a relation between noise intensity in the air mass flow sensor and turbine speed from this data. Fair results are obtained for the noise in p_{im}, p_{em} and n_{trb}.

Applying (2.1) to describe the noise in the air mass flow sensor does not give as good results as for the other signals.

2.2.1 Variations due to environment

It is difficult to extract the actual noise in a process, and in this thesis the noise in air mass flow sensor is described as a lumped parameter. This parameter consists of the noise and the model uncertainties, i.e. the noise is a way to model the incorrectness of the model. Read more about modelling and using noise in [And05].

How does the environment affect the noise intensity? This is not obvious due to the complexity of the system, but a first guess is that a more complex system will be noisier and have more model uncertainties. In this chapter this is investigated by comparing the noise variance from three different environments. The measurements in these environments have the purpose to isolate the origin of the noise in the sensor. The environments where the sensor is placed are:

- A straight pipe placed in a test apparatus.

- The intake manifold placed in a test apparatus.

- The intake manifold placed in a truck.

In the first set-up the noise observed in the measured signal is assumed to originate from the sensor itself since the air mass flow in the pipe is not disturbed by the pipe. Therefore this set-up gives an indication of the magnitude of the measurement noise.

In the second set-up the noise observed in the measured signal is a mix of measurement noise and system noise. The system noise in this set-up originate from the shape of the intake manifold.

The third set-up is quite similar to the second with the difference that here the system noise consists of contributions from both the shape of the intake manifold and the vibrations etc. from the vehicle.

2.2.2 Variations due to air mass flow

As stated in Section 2.2 a weak quadratic relation is observed between measurement noise intensity and turbine speed, i.e. the air mass flow. In this thesis this potential relation is captured in a different way. It is now possible to characterize the noise in all operating points. The approach in this thesis

is to extract the noise sequences for each operating point, and from these sequences calculate the Q- and R-matrices in the Kalman filter, see Section 2.4.

2.3 Experimental set-up

The experimental set-up consists of two different pipes, a straight millboard pipe and an intake manifold. With the straight pipe one experiment is performed in a test apparatus and with the intake manifold two experiments are performed, one in a test apparatus and one in a truck. These experiments are further described in the following sections. The test apparatus experiments were performed by Mats Jennische at Scania who provided us with this data.

2.3.1 Test apparatus

The test apparatus consists of a fixed fan and a pipe to make sure that the environments examined, i.e. the pipe and the intake manifold, are placed in as smooth and laminar[1] flow as possible.
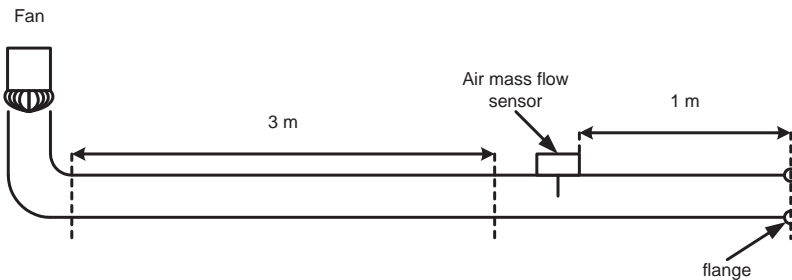
Figure 2.1: Test apparatus with the straight millboard pipe connected.

Straight pipe

In this set-up a straight four inches millboard pipe is connected to the fan. To smoothen the flow further there is a flange at the end of the pipe. The set-up can be seen in Figure 2.1.

Intake manifold

In this experimental set-up the straight pipe is replaced by the intake manifold.

---

[1]Laminar flow is the fluid is moving in smooth layers in the object.

2.3.2   Vehicle

The final experiment is performed with the intake manifold in a truck. Here the air mass flow is determined by the speed of the compressor and not by the fan, as in the test bed experiment. The conditions in the vehicle are quite different from those in the test apparatus, as stated in Section 2.2.1. In the truck there is e.g. an air-filter just prior to the intake manifold, which makes the air more turbulent than a straight pipe.

2.4   Treating and collecting data

This section describes how the data is selected and processed. Obtaining good results are highly dependent on good data sets. Many data sets used in this thesis contain bad or missing data. Ljung extensively describes the theory explaining data selection and processing in [Lju99].

2.4.1   Data collection

The data is collected from a test apparatus and from a Scania R124 diesel truck. The noise is extracted from the air mass flow signal at each stationary operating point. From this information the intensity at the different operating points is calculated.

2.4.2   Data selection

In the data selection, the following criteria are considered:

1. To make sure that only the noise is examined the sequence need to be stationary, see Section 2.5.

2. To achieve data from which it is possible to estimate a relation similar to the one proposed in [Swa05], sequences from several different operating points in the working area of the engine have to be used.

The first criterion give rise to problems since the noise in the transients is not taken into consideration.

2.4.3   Data processing

Due to the fact that the data acquisition equipment is not perfect, single values or portions of data may be missing. This is because of malfunctions in the sensors or communication links. Certain measured values may also be in obvious error due to measurement failure. These bad data can have a substantial negative effect when using the sequence in e.g. the frequency analysis in Section 2.5.

Some of the sequences used in the estimation in Section 2.5 contain missing data in the input signal, i.e. the turbine speed. These data sets are treated using one of the methods proposed in [Lju99]. The method used in this thesis is to replace the missing data with the mean value of the preceding values in the current data sequence. This way to treat missing or bad data works in this case since the data needing correction is stationary and works as input to the model.

To isolate the noise in the signal, offsets and trends have to be removed. The offset is removed by subtracting the mean value of the signal from the signal, and the trends is removed in a similar way by adjusting a straight line to the signal and subtract it from the signal.

2.5 Frequency analysis

To get a better understanding of the properties of the noise in the air mass flow sensor a frequency-domain method is used. The fundamental idea behind these methods is to approximate the frequency content in the signal. Signals that are smooth enough, discrete as well as continuous, can be described as functions of *cosinus* and *sinus* components. This information will in this case describe the characteristics of the noise in the sensor.

2.5.1 Theory

The (power) spectrum of a discrete-time signal describes the frequency contents of the signal. For a weakly stationary stochastic process, the spectrum is defined as the Fourier transform of the covariance function

$$\Phi_{xx}(\omega) = T \sum_{n=-\infty}^{\infty} R(nT)e^{-i\omega nT}. \tag{2.2}$$

Obviously it is necessary to investigate if our processes really are weakly stationary processes. One has to recall that this is a theoretical property that not easily applies to measured signals. This implies that this investigation only makes it probable that the processes are weakly stationary, and this investigation is not a proof whatsoever. The following theorem will help in the analysis.

Theorem 2.1. *A process is weakly stationary if*

$$m(t) = m \tag{2.3}$$
$$R(t_1, t_2) = R(t_1 - t_2), \tag{2.4}$$

where m is the mean value and R is the auto correlation function, holds.

This theorem states that a weakly stationary process demands a time independent mean value (2.3) and a time independent auto correlation function

(2.4).

Some of the sequences in the measurements of the air mass flow in the environments presented in 2.3 appear to have time independent auto correlation function, see Figure 2.2. One observation is that the auto correlation looks whiter in those cases where the sensor is situated in a more complicated environment. Note that the auto correlation function for white noise[2] is just an impulse:

$$R(\tau) = R_0\delta(\tau) \tag{2.5}$$
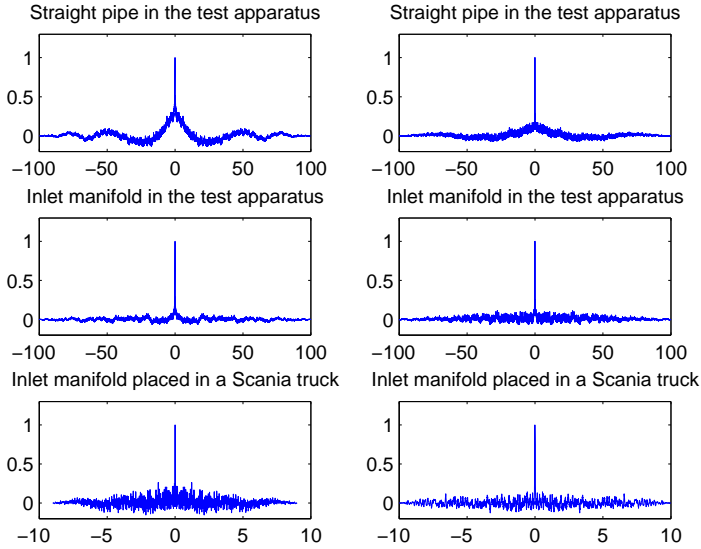
Figure 2.2: Auto correlation functions for the sequences. In the left column the air mass flow is approximately 0.35 kg/s and in the right column the air mass flow is approximately 0.20 kg/s. The top row is a straight pipe and the second row is the inlet manifold in the test apparatus. The bottom row is the inlet manifold in a truck. Note that the measurements in the test apparatus are ten times longer than in the Scania truck.

The chosen sequences prove to be approximately Gaussian with a time independent mean value close to zero. The statement about the mean value is natural though, since the chosen sequences are stationary in turbine speed, and their mean values and trends are removed. In other words, the sequences are chosen to fulfil the demands concerning the mean value.

Regarding the approximation that the sequences are Gaussian, see Figure 2.3. In these figures, histograms for the sequences and the superimposed

---

[2]White noise is noise that has its energy equally distributed over all frequencies.
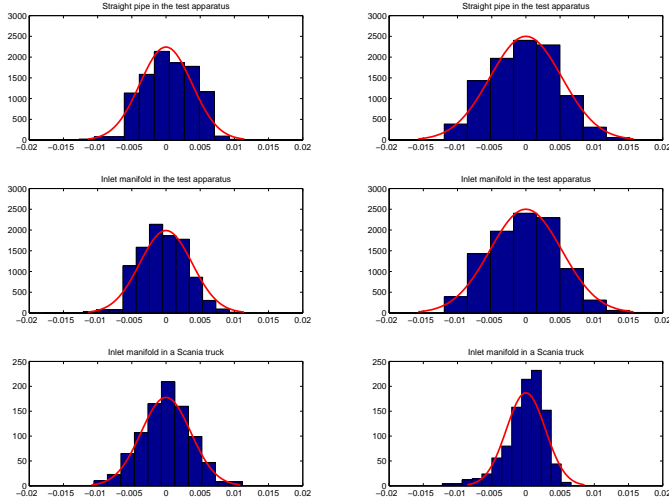
Figure 2.3: Histograms for the sequences and the superimposed normal density. In the left column the air mass flow is approximatley 0.35 kg/s and in the right column the air mass flow is approximatley 0.20 kg/s. The top row is a straight pipe and the second row is the inlet manifold in the test apparatus. The bottom row is the inlet manifold in a truck.

normal density show that the Gaussian approximation is reasonable. For completeness, a theorem about gauss processes is stated below.

Theorem 2.2. *A weakly stationary Gaussian process is always strictly stationary.*

This means that Equation (2.2) holds.

The data only has a finite number of samples

$$y(nT), n = 0, 1, 2, \ldots, N-1. \tag{2.6}$$

If the frequency content in this finite sequence is to be investigated another approach has to be used. This is due to the fact that it is impossible to calculate the spectrum for an observed (finite) signal. Instead sequence (2.6) is estimated. This is done by looking at the discrete-time Fourier transform of the truncated signal and its normalized absolute value in square. That is

$$Y_T^{(N)}(e^{i\omega T}) = \sum_{n=0}^{N-1} y(nT)e^{-i\omega nT} \tag{2.7}$$

$$\hat{\hat{\Phi}}_N(\omega) = \frac{1}{NT} \left| Y_T^{(N)}\left(e^{i\omega T}\right) \right|^2. \tag{2.8}$$

The estimate (2.8) is called the periodogram of (2.6) and describes the contribution from the frequency

$$\omega = \frac{2\pi n}{NT} \tag{2.9}$$

to the decomposition of sequence (2.6).

2.5.2   Method

There are several ways to perform the spectral analysis and two well known methods are Welch's method and Blackman-Tuckey's method. In this thesis the spa function in MATLAB[3] is used, which in turn uses the Blackman-Tuckey's approach. This is further discussed in [FG01], and for a periodic signal in [Lju99].

The signals at hand will give a spectral density that implies low frequent contents in the noise for the air mass flow sensor, see Figure 2.4. The reason for the fluttering is that the variance does not decrease with an increasing number of samples, see [FG01]. Note that Figure 2.4 does not distinguish measurement noise and process noise.

2.6   Filter analysis

In Chapter 4 a Kalman-observer is calculated. Calculating an observer with Kalman theory requires knowledge of the disturbances present in the system. The disturbances are of two kinds, measurement disturbance and system disturbance. The measurement disturbance, or measurement noise, is noise that originates from variations or inaccuracy in the sensor equipment and does not affect the system. The system noise, on the other hand, is noise that originates from phenomena not modelled or disturbances that affect the system. These disturbances are often hard to describe accurately and they are seldom white noise. When the disturbances are Gaussian white noise, it can be proved that the Kalman filter is optimal among all filters, linear as well as non-linear, consult e.g. [FG01]. To handle this problem the noise can be modelled and included in the model. Non-white noise can sometimes be modelled as white noise through a stable linear filter, see Figure 2.5. v is the system or measurement noise, w is white noise and H is the filter.
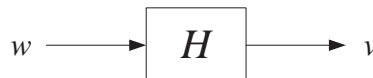
Figure 2.5: White noise w through a filter H gives the sensor noise v.

---

[3]MATLAB and SIMULINK are registered trademarks of The MathWorks, Inc.
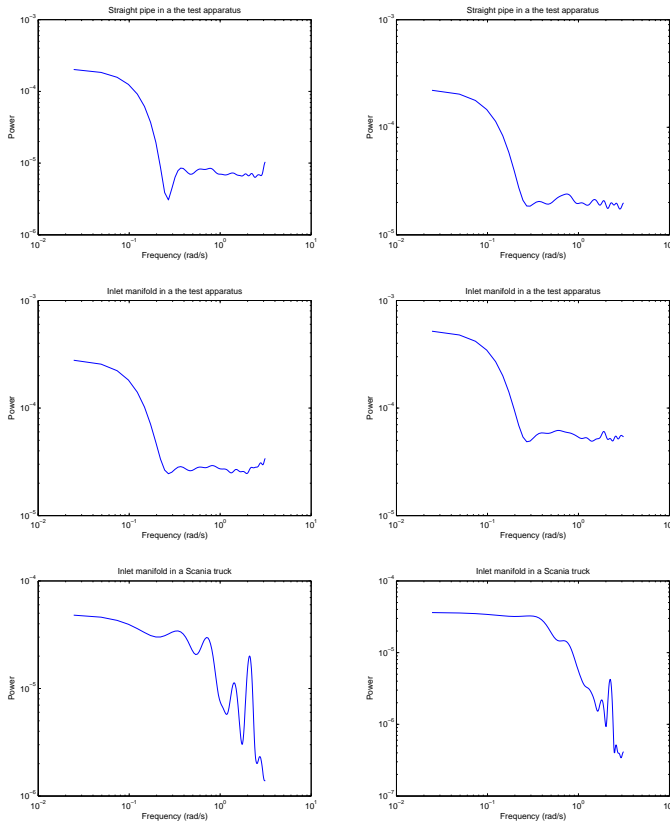
Figure 2.4: Spectrum for the sequences. In the left column the air mass flow is approximately 0.20 kg/s and in the right column the air mass flow is approximately 0.35 kg/s. The top row is a straight pipe and the second row is the inlet manifold in the test apparatus. The bottom row is the inlet manifold in a truck.

As stated in Section 2.5 the noise is a realization of a stationary process. This means that the auto correlation function of v becomes

$$R_v(\tau) = \int_{-\infty}^{\infty} \int_{-\infty}^{\infty} h(\tau_1)h(\tau_2)R_w(\tau - \tau_1 + \tau_2)d\tau_1 d\tau_2 \qquad (2.10)$$

and the spectral density

$$\Phi_v(\omega) = |H(\omega)|^2 \, \Phi_w(\omega). \qquad (2.11)$$

Looking at (2.11) one realize that the assumption that it is only the intensity of the white noise that varies with the turbine speed, is not quite so simple. The reason for this is the difficulties to say whether it is the intensity of the white noise or the filter that varies with the turbine speed. To investigate this, a system identification procedure is applied to the noise sequences.

2.6.1   Black-box models

In some cases the system cannot be modelled through physical derivation due to its unknown structure or because it is to complex to sort out the physical relations. In these cases it is suitable to use standard models that through experience is known to handle many different kinds of system dynamics. Linear systems are the most common among these standard models.

Transfer function models

Normally these models are derived in discrete time, since the data used is sampled and therefore discrete. To get a model in continuous time the discrete model can be transformed. A general linear model in discrete time can be written as

$$y(t) = \eta(t) + w(t). \qquad (2.12)$$

Where $w(t)$ is a disturbance term and $\eta(t)$ is the output without disturbance. This output can be written as

$$\eta(t) = G(q, \theta)u(t). \qquad (2.13)$$

Where $G(q, \theta)$ is a rational function of the displacement operator q,

$$G(q, \theta) = \frac{B(q)}{F(q)} = \frac{b_1 q^{-n_k} + b_2 q^{-n_k-1} + \cdots + b_{n_b} q^{-n_k-n_b+1}}{1 + f_1 q^{-1} + \cdots + f_{n_f} q^{-n_f}}. \qquad (2.14)$$

With this (2.13) can be written as the difference equation

$$\eta(t) + f_1\eta(t - T) + \cdots + f_{n_f}\eta(t - n_f T) = \\ b_1 u(t - n_k T) + \cdots + b_{n_b} u(t - (n_b + n_k - 1)T). \qquad (2.15)$$

The disturbance term can be treated in the same way with

$$w(t) = H(q, \theta)e(t) \tag{2.16}$$

and

$$H(q, \theta) = \frac{C(q)}{D(q)} = \frac{1 + c_1 q^{-1} + \cdots + c_{n_c} q^{-n_c}}{1 + d_1 q^{-1} + \cdots + d_{n_d} q^{-n_d}}, \tag{2.17}$$

where $e(t)$ is white noise.

Now the model (2.12) can be written as

$$y(t) = G(q, \theta)u(t) + H(q, \theta)e(t) \tag{2.18}$$

where θ contains the coefficients a_i, b_i, c_i and f_i in the transfer functions. This is called the *Box-Jenkins model* and is described by the five "structure" parameters n_b, n_c, n_d, n_f and n_k. Box-Jenkins is the most general form of the linear black-box models and can be simplified in a numerous different ways to suit other more specific systems. One of these is the AR-process (autoregressive), which is achieved by setting $b_i = c_i = f_i = 0, i \neq 0$. This means that (2.18) becomes

$$y(t) = \frac{1}{D(q)} e(t). \tag{2.19}$$

The reasons for choosing the AR-process in this thesis are that it is simple and easy to estimate.

2.6.2 Results

The procedure is performed with System Identification Toolbox in MATLAB. This resulted in the model choice of a first order AR-model

$$H = \frac{1}{1 + aq^{-1}}. \tag{2.20}$$

With the idea that the filter is dependent on the turbine speed, Equation (2.20) becomes

$$H(n_{trb}) = \frac{1}{1 + a(n_{trb})q^{-1}}. \tag{2.21}$$

In Figure 2.6 the result of the filter analysis is presented. As can be seen it is hard to state any relation between the turbine speed and the filter. The reasons for this are the big differences in the a-values for different turbine speeds.

The data in this filter analysis is selected and treated as proposed in Section 2.4.
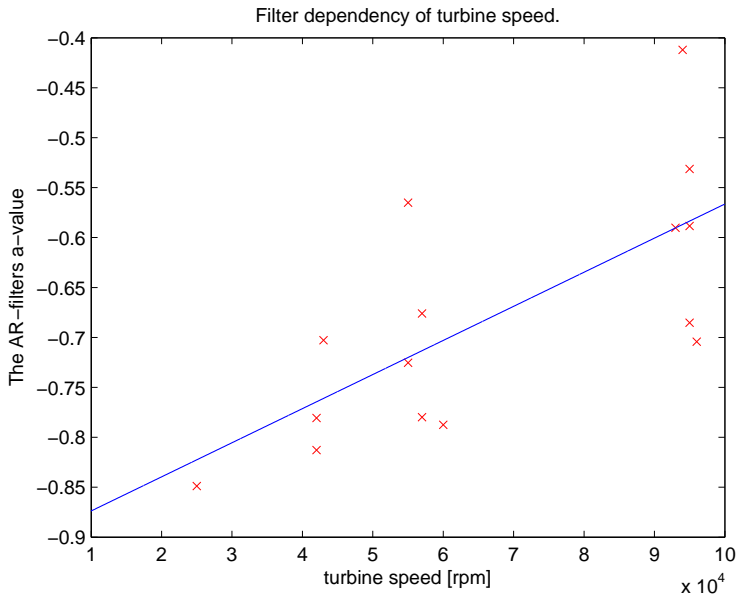
Figure 2.6: The filter dependence of the turbine speed, n_{trb}.

Chapter 3

Modelling

To further improve the observer the number of signals used for feedback can be increased. In [Swa05] the intake manifold pressure, the exhaust manifold pressure and the turbine speed are used for feedback in the observer. Other sensor signals possible to use for feedback are the signals from the air mass flow sensor and the temperature sensor in the intake manifold. To use these signals for feedback they have to be modelled. The air mass flow is already in the model but the intake manifold temperature is not, so the model needs to be extended with models and states for the temperature.

Some parts of the existing mean value engine model are also improved and some new parts are added. The following parts are further investigated in this thesis:

- Temperature drop over the intercooler.

- Temperature states in the intercooler, intake manifold and exhaust manifold.

- Temperature and pressure dynamics in the EGR system.

- Heat exchange in the exhaust manifold.

- Temperature and pressure dynamics in the exhaust system due to the exhaust brake.

- Temperature sensor dynamics.

3.1   Model structure

The model is a MVEM with sub models for each subsystem. A MVEM describes the average behaviour of the engine, which means that the signals, parameters and variables that are considered are averaged over one or several

cycles[1]. The subsystems are the compressor, intercooler, intake manifold, combustion, exhaust manifold, EGR-system, VGT and exhaust system with an exhaust brake. The components, or sub models, added to the existing model are described in this section. To make the model in this thesis complete, the existing model is briefly described here as well. The model is implemented in MATLAB/SIMULINK and can easily be altered with more or less components or dynamics. Figure 3.1 shows how the different components are connected to each other and where the model dynamics exist.

---

[1]One cycle for a four stroke engine is two revolutions of the crank shaft. For a thorough description of the four stroke cycle consult Nielsen and Eriksson in [LN04].
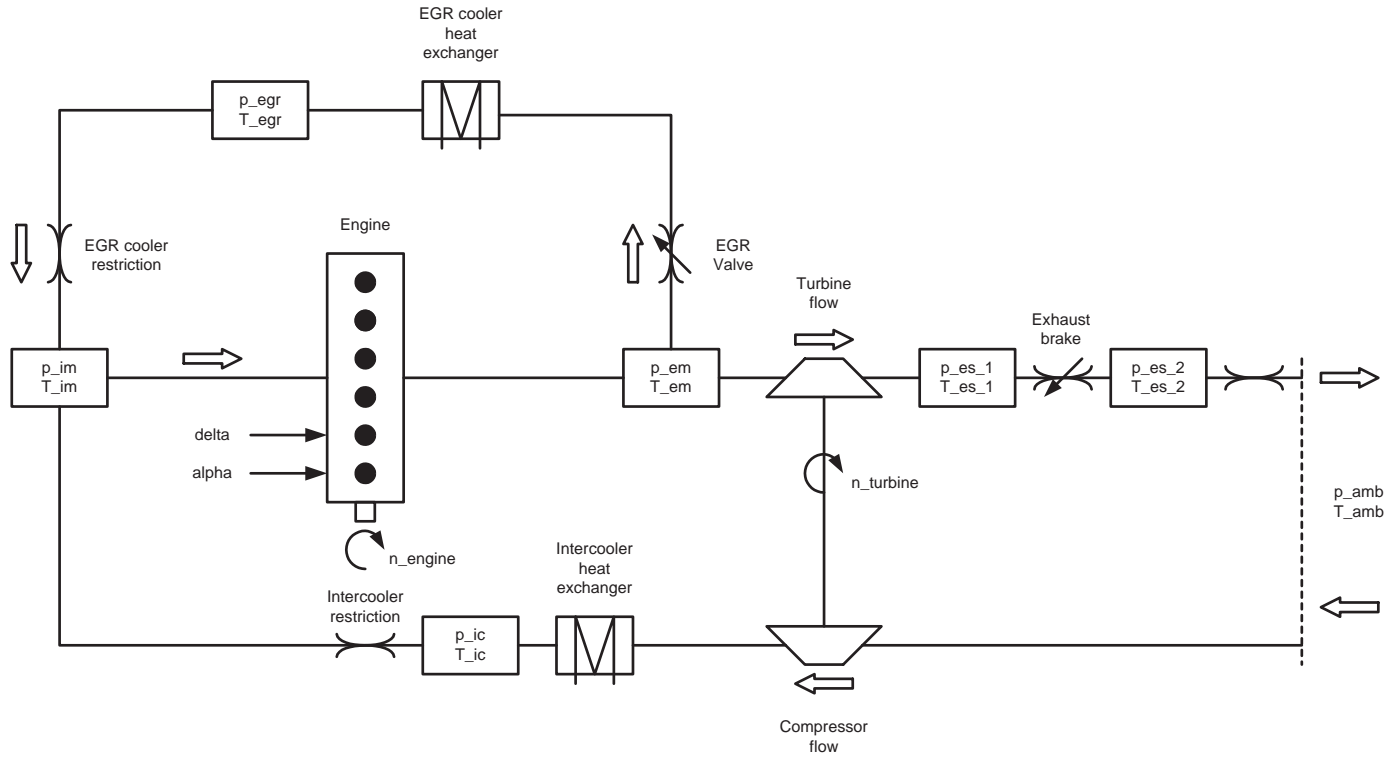
Figure 3.1: System overview.

3.2 Compressor

The compressor is driven by the turbine shaft which is attached to the VGT. It increases the density and temperature of the air flowing into the engine. This will in turn not only give a higher efficiency and power output from the engine, but also a higher temperature in cylinders and the exhaust gases. The compressor has not been treated in this thesis, but the equations will be presented for completeness.

The efficiency and the flow out of the compressor are described by static maps with pressure ratio over the compressor and turbine speed as inputs. These maps are supplied by the manufacturer.

$$W_{cmp} = f_{W_{cmp}}\left(\frac{p_{cmp}}{p_{amb}}, n_{trb}\right) \tag{3.1}$$

$$\eta_{cmp} = f_{\eta_{cmp}}\left(\frac{p_{cmp}}{p_{amb}}, n_{trb}\right) \tag{3.2}$$

$$T_{cmp} = T_{amb}\left(1 + \frac{\Pi_{cmp}^{\frac{\gamma_{air}-1}{\gamma_{air}}} - 1}{\eta_{cmp}}\right) \tag{3.3}$$

where $\Pi_{cmp} = \frac{p_{cmp}}{p_{amb}}$ is the pressure ratio over the compressor and $\gamma = \frac{c_p}{c_v}$ is the ratio of the specific heats.

3.3 Intercooler model

To get an even higher power output and efficiency of the engine an intercooler is added to cool the charged air. This will increase the density of the air, and by that increase the amount of air flowing into the cylinders. A higher density of the air makes it possible to inject a higher amount of fuel. Consult e.g. [LN04] for a thorough discussion.

The existing intercooler model consists of a control volume and a restriction. The control volume only contains a state for the pressure and will be complemented with a state for the temperature as well. A heat exchanger model will also be added. The model choices are made in accordance with [Hol05].

3.3.1 Control volume

The control volume is a two state control volume with states for pressure, p, and temperature, T. The control volume has a fixed volume, V, and the change of mass within the control volume is determined by the air mass flow in and out of the control volume. Within the control volume the energy is conserved and stored. The energy transfers to or from the control volume through the air mass flow, $\dot{m}$, and by the heat transfer, $\dot{Q}$. Here a derivation

of the differential algebraic equations follows. For more details see [LN04] and [Hol05].

The rate of the mass change in the control volume is given by

$$\frac{dm}{dt} = \dot{m}_{in} - \dot{m}_{out} \tag{3.4}$$

and the change of the internal energy is given by

$$\frac{dU}{dt} = \dot{H}_{in} - \dot{H}_{out} - \dot{Q}. \tag{3.5}$$

To facilitate the modelling and to keep the model from becoming to complex, the following assumptions are made:

- The gas inside the control volume is ideal,

$$pV = mRT \tag{3.6}$$

- c_p and c_v are constant,

$$R = c_p - c_v. \tag{3.7}$$

- The temperature of the gas flowing out is the same as that in the control volume,

$$T_{out} = T. \tag{3.8}$$

With these assumptions the pressure can be determined from the ideal gas law, Equation (3.6), and the temperature can be determined from the internal energy and the mass through

$$U = mu(T) = [c_v - constant] = mc_vT. \tag{3.9}$$

The enthalpy flows are given by

$$\dot{H}_{in} = \dot{m}_{in}c_pT_{in} \qquad and \qquad \dot{H}_{out} = \dot{m}_{out}c_pT_{out}. \tag{3.10}$$

The pressure differential is achieved by differentiating the ideal gas law (3.6) which, when the temperature is allowed to change, becomes

$$V\frac{dp}{dt} = RT\frac{dm}{dt} + mR\frac{dT}{dt}. \tag{3.11}$$

Inserting (3.4) and eliminating the mass with the ideal gas law (3.6), Equation (3.11) becomes

$$\frac{dp}{dt} = \frac{RT}{V}\left(\dot{m}_{in} - \dot{m}_{out}\right) + \frac{p}{T}\frac{dT}{dt}. \tag{3.12}$$

The temperature differential is achieved by differentiating the internal energy (3.9) which gives the relationship

$$\frac{dU}{dt} = \frac{dm}{dt}c_v T + mc_v \frac{dT}{dt}. \qquad (3.13)$$

Combining (3.4), (3.5), (3.10) and (3.13) yields

$$c_v T \left(\dot{m}_{in} - \dot{m}_{out}\right) + mc_v \frac{dT}{dt} = \dot{m}_{in} c_p T_{in} - \dot{m}_{out} c_p T_{out} - \dot{Q}. \qquad (3.14)$$

Rearranging the terms in (3.14) and inserting (3.6), (3.7) and (3.8) result in the following temperature differential

$$\frac{dT}{dt} = \frac{RT}{pVc_v} \left(\dot{m}_{in} c_v \left(T_{in} - T\right) + R \left(T_{in}\dot{m}_{in} - T\dot{m}_{out}\right) - \dot{Q}\right). \qquad (3.15)$$

In this thesis the heat transfer is assumed to be zero on the intake side but not on the exhaust side. The heat transfer on the exhaust side will be modelled in accordance with Eriksson in [Eri02] and will be presented in Section 3.6.1. In both cases $\dot{Q} = 0$.

3.3.2   Restriction

The intercooler restriction is modelled as an incompressible restriction since the gas velocity through the intercooler is slow. The restriction model has the pressure after the compressor and the pressure after the intercooler as inputs and the mass flow through the intercooler as output. The pressure loss over the restriction is described with one parameter H_{res}, the restriction coefficient, see [LN04].

The equations for the intercooler restriction are

$$\Delta p_{res} = p_{us} - p_{ds} = H_{res} \frac{T_{us} W_{res}^2}{p_{us}} \qquad \Rightarrow \qquad (3.16)$$

$$W_{res} = \sqrt{p_{us} \frac{\Delta p_{res}}{H_{res} T_{us}}}. \qquad (3.17)$$

Since the derivative of (3.17) with respect to Δp_{res} approaches infinity as Δp_{res} approaches zero, the function is linearized to

$$W_{res} = \sqrt{\frac{p_{us}}{H_{res} T_{us}}} \frac{\Delta p_{res}}{\sqrt{p_{lin}}} \qquad (3.18)$$

for $0 \leq \Delta p_{res} \leq p_{lin}$. For causality, the simplification that flow only runs in forward direction in the model has been made, W_{res} is set to 0 for $\Delta p_{res} \leq 0$.

3.3.3 Heat exchange

In the intercooler there are two mass flows present, the air mass flow and the cooling air mass flow. In combustion engines the flow rate of the cooling air, $\dot{m}_{cool}$, is greater than the mass flow, $\dot{m}_{air}$, i.e. $\dot{m}_{cool} > \dot{m}_{air}$. In [LN04] by Nielsen and Eriksson the following equation for the temperature after the intercooler is proposed

$$T_{ic} = T_{cmp} - \epsilon_{ic}\left(T_{cmp} - T_{cool}\right) \tag{3.19}$$

where

$$T_{cool} = T_{amb} \tag{3.20}$$

and

$$\epsilon_{ic} = k_{ic}. \tag{3.21}$$

The result of the estimation of the parameters can be seen in Section 6.1.

3.4 Intake manifold

The intake manifold connects the inlet system with the EGR system and feeds the cylinders with a mixture of fresh air and EGR gases.

The intake manifold is modelled as a control volume with two pressure states, one for oxygen and one for inert gases, and one common temperature state. The separation between inert gases and oxygen is done to get a better estimation of the lambda[2] value. This separation was initially done in [Swa05]. Only one temperature state is needed due to the fact that the gases are mixed before the control volume and are considered completely mixed inside the control volume. In this thesis the mixing of EGR gas and supercharged air takes place before the intake manifold. This is a simplification since the EGR gases are actually mixed with the supercharged air in the middle of the intake manifold.

3.4.1 Gas mixing

The gas mixture in the control volume will be described by new specific heat capacities, c_p and c_v. Here follows a presentation of these new quantities.

$$c_{v,im} = \frac{c_{v,air}\dot{m}_{ic} + c_{v,egr}\dot{m}_{egr}}{\dot{m}_{im,in}} \tag{3.22}$$

$$R_{im} = \frac{R_{air}\dot{m}_{ic} + R_{exh}\dot{m}_{egr}}{\dot{m}_{im,in}} \tag{3.23}$$

---

[2]The lambda value is defined as $\lambda = \frac{(m_{air}/m_{fuel})}{(m_{air}/m_{fuel})_s}$ were the index s refers to a stoichiometric combustion reaction. Read more in e.g. [LN04]

with

$$\dot{m}_{im,in} = \dot{m}_{ic} + \dot{m}_{egr} \tag{3.24}$$

and T_{im} becomes

$$T_{im} = \frac{T_{ic}c_{v,air}\dot{m}_{ic} + T_{egr}c_{v,egr}\dot{m}_{egr}}{c_{v,im}\dot{m}_{im,in}}. \tag{3.25}$$

3.4.2   Control volume

The control volume has two pressure states, one for oxygen and one for inert gases, and one temperature state. These pressure and temperature states are modelled as described in Section 3.3.1.

3.5   Combustion

The mixture of air and fuel is injected into the combustion chamber, i.e. the cylinder, under high pressure. In the cylinder, the air and fuel mixture is burned. This liberates the energy in the fuel and the piston is forced down by the burned gases. These gases have high temperatures and high pressures.

   The combustion has not been treated in this thesis, but the equations will be presented for completeness. Read more about the combustion in [Elf02].

$$W_{eng,in,tot} = \eta_{vol}\frac{V_d N_{eng} p_{im}}{120 R_{im} T_{im}} \tag{3.26}$$

$$\eta_{vol} = f_{\eta_{vol}}\left(N_{eng}, \frac{p_{im}}{T_{im}R_{im}}\right) \tag{3.27}$$

$$T_{em} = t_{im} + \frac{Q_{LHV}f_{T_{em}}\left(W_{fuel}, N_{eng}\right)}{c_{p,exh}\left(W_{eng,in} + W_{fuel}\right)} \tag{3.28}$$

where

$$W_{fuel} = \frac{\delta N_{eng} N_{cyl}}{120}. \tag{3.29}$$

3.6   Exhaust manifold

The exhaust gases flow into the exhaust manifold after combustion. The exhaust manifold is modelled as a control volume with one temperature state and two pressure states just like the intake manifold. A significant difference between the intake manifold and the exhaust manifold is the heat transfer. In the intake manifold the heat transfer is assumed to be zero and here it is modelled as described in 3.6.1.

3.6.1   Heat transfer

The exhaust gases leaving the cylinders have high temperatures in comparison to the ambient temperature. This results in a temperature drop of the exhaust gases when they pass through the exhaust pipe. This phenomenon is described in [Eri02]. The temperature drop in the fluid is modelled as a one dimensional flow with the outlet temperature T_{out}

$$T_{out} = T_{wall} + (T_{in} - T_{wall}) \, e^{-\frac{h(W)A}{Wc_p}} \qquad (3.30)$$

where T_{wall} is the pipe wall temperature, T_{in} intake temperature, $h(W)$ heat transfer coefficient, A pipe wall area, and W mass flow. Eriksson compared three different models, two stationary and one dynamic. The choice in this thesis is a stationary model without pipe wall conduction along the flow direction and where all heat transfer modes in Equation (3.32) are lumped together to one total heat transfer coefficient h_{tot}. Hence the heat transfer is from the gas to constant ambient conditions with a constant heat transfer coefficient and with $T_{wall} = T_{amb} + T_{amb,corr}$ the model can be summarized as

$$T_{out} = (T_{amb} + T_{amb,corr}) + (T_{in} - (T_{amb} + T_{amb,corr})) \, e^{-\frac{h_{tot}A}{Wc_p}}$$
$$(3.31)$$

where

$$\frac{1}{h_{tot}} = \frac{1}{h_{cv,i}} + \frac{1}{h_{cv,e} + h_{cd,e} + h_{rad}} \qquad (3.32)$$

and $T_{amb} + T_{amb,corr}$ is the adjusted ambient temperature. T_{amb} is the temperature outside the vehicle, but near the engine the temperature is a bit higher which is described by $T_{amb,corr}$. In our case Equation (3.31) can be rewritten as

$$T_{em,cooled} = (T_{amb} + T_{amb,corr}) + (T_{em} - (T_{amb} + T_{amb,corr})) \, e^{-\frac{h_{tot}A}{Wc_p}}$$
$$(3.33)$$

where $T_{em,cooled}$ is the temperature of the gas flowing into the EGR system. The approximation that $T_{wall} = T_{amb} + T_{amb,corr}$ can be motivated by the fact that the wall conduction coefficient is so large that the wall can be approximated to have the same temperature as the surroundings. h_{tot} is normally used as tuning parameter but since A is hard to estimate accurate the tuning parameter in this thesis will be $h_{tot}A$.

The choice of a stationary model can be motivated by the fact that the existing model already catches the dynamics well but models the temperature of the exhaust gases too high in comparison to the measured temperatures. The result of the estimation of the parameters can be seen in Section 6.3.

3.6.2   Vontrol volume

The control volume has two pressure states, one for oxygen and one for inert gases, and one temperature state. These pressure and temperature states are modelled as described in Section 3.3.1.

3.7   VGT

To be able to control the amount of air fed into the cylinders and the EGR flow a VGT is used. The VGT is driven by the exhaust gases which force it to rotate. The VGT is connected to the compressor which feed compressed air into the intake manifold. The VGT is described in [Elf02], and the equations will just be described in a few words.

The pressure ratio between the exhaust manifold and the exhaust system, the turbine speed together with the position of the VGT describe the flow in the map 3.34. The temperature after the VGT is given by the Equation 3.35.

$$W_{VGT} \quad = \quad f_{W_{trb}}\left(\frac{p_{em}}{p_{es}}, n_{trb}, u_{vgt}\right) \tag{3.34}$$

$$T_{VGT} \quad = \quad \left(1 + \eta_{trb}\left(\left(\frac{p_{es}}{p_{em}}\right)^{\frac{\gamma_{exh}-1}{\gamma_{exh}}} - 1\right)\right) T_{em} \tag{3.35}$$

3.8   Exhaust system

This system consists of a silencer and an exhaust pipe in series. An exhaust brake is located immediately before the silencer. The exhaust system is modelled as two control volumes and two restrictions, one variable restriction for the exhaust brake and one fix restriction for the exhaust pipe. The control volume before the exhaust brake is small and the control volume after the exhaust brake is large. This means that the states in the control volume before the exhaust brake will be much faster than the states after the exhaust brake. Because of this the total system will be stiff[3]. In previous models the exhaust system are modelled without the exhaust brake and they have a single control volume.

3.8.1   Control volumes

The control volumes are modelled as described in Section 3.3.1.

---

[3]Differential equations with a significant dispersion between the time constants

3.8.2 Restrictions

The fix restriction is modelled as an incompressible restriction and is therefore modelled as described in Section 3.3.2. The variable restriction on the other hand is modelled as a compressible restriction and will be further presented below.

Compressible restriction

The exhaust brake is modelled as a compressible restriction since the gas velocity through this restriction is high, see [LN04].

The mass flow depends on the opening area, the density before the contraction and the pressure ratio over the contraction. The mass flow through a contraction like this is

$$\dot{m} = \frac{p_{us}}{\sqrt{RT_{us}}} \cdot A_{eff} \cdot \Psi\left(\frac{p_{ds}}{p_{us}}\right) \tag{3.36}$$

where

$$A_{eff} = A \cdot C_D. \tag{3.37}$$

A is the inner area of the pipe and C_D is a discharge coefficient that depends on the shape of the flow area. A_{eff} is the effective flow area and is smaller than A due to the contraction of the flow described by C_D. $\Psi(\frac{p_{ds}}{p_{us}})$ and $\frac{p_{us}}{\sqrt{RT_{us}}}$ describe the velocity and density in terms of intake conditions.

A_{eff} and Ψ are modelled as lookup tables and the derivation of these will not be presented in this thesis.

3.9 EGR system

In order to lower the NO_x formation a portion of the exhaust gases are recirculated to the intake manifold. This reduces the peak temperature, and by that, NO_x formation. Not only the NO_x will decrease, but also the fuel consumption with increased EGR flow. To avoid misfire, the EGR flow cannot be allowed to get to high. The EGR system consists of a valve and an EGR cooler.

The current model contains a control volume and a restriction. The control volume only contains a pressure state. In this thesis the model will be extended with a temperature state as well. The heat exchange in the EGR is modelled in two steps. These steps are the valve and the EGR cooler. The model choices are made in accordance with [Eri04].

3.9.1   Valve

The temperature drop over the valve is small and measurements are unreliable during low gas flows in the EGR system. The isentropic model proposed by Ericson in [Eri04] proved hard to validate. Instead, Ericson chose not to model any temperature drop over the valve. Despite this the temperature drop over the valve is modelled in this thesis.

$$T_{valve} = \left(\frac{p_{valve}}{p_{exh}} \right)^{\frac{\gamma-1}{\gamma}} T_{exh} \qquad (3.38)$$

3.9.2   EGR cooler

The efficiency of the EGR cooler is hard to model because of difficulties in temperature measurements. Therefore, a constant efficiency is used in this thesis as well.

$$T_{EGR} = T_{valve} - \epsilon_{egr} \left(T_{valve} - T_{EGR} \right) \qquad (3.39)$$
$$\epsilon_{egr} = k_{egr} \qquad (3.40)$$

The result of the estimation of the parameters can be seen in Section 6.2.

3.9.3   Control volume

The control volume in the EGR system is modelled in the same way as in Section 3.3.1.

3.9.4   Restriction

The EGR restriction is modelled as an incompressible restriction, see Section 3.3.2. The result of the estimation of the parameters can be seen in Section 6.2.

3.10   Temperature sensors

Temperature sensors have slow dynamics and it can therefore be hard to compare measured and simulated signals when the temperature changes fast. Therefore a model for the temperature sensors is included in the model. The temperature sensors are modelled as first order systems.

$$T_{sensor} = \frac{1}{\frac{1}{T}s + 1} T_{modelled} \qquad (3.41)$$

T is the time constant of the temperature sensor, $T_{modelled}$ the actual temperature and T_{sensor} the temperature measured by the sensor. The thermal

element in the temperature sensor has a diameter of approximately 1 mm and this will, according to [Eri02], result in a value of about 0.6 seconds for the time constant, T. This applies to the case when the sensor is situated in flowing air.

Chapter 4

Observer design

An observer can have several different applications in a model. It can for example be used for diagnosis of sensors and actuators and to predict signals not measured. In this thesis, the primary application of the observer will be to improve the state estimates in the model using sensor fusion between measured and modelled signals. Sensor fusion deals with the problem to weight the different signals together. This is conducted by the Kalman filter, which is a linear filter. Due to the nonlinear dynamics of the system a more general form of the Kalman filter is used, the constant gain extended Kalman filter.

4.1 Kalman filter and observer

During the Second World War, Norbert Wiener implemented the Wiener filter in radar applications. The Wiener filter needs stationary and scalar signals, but it is the optimal filter to extract the interesting signal from a noisy signal.

In 1960 R.E. Kalman and R.S. Bucy derived the Kalman filter which is a generalization of the Wiener filter. One limitation of the Kalman filter is that the relation between the measured signal and the interesting signal is described in state-space form which limits the filter to linear systems.

4.1.1 Linear model

As mentioned in Section 4.1 the system has to be in general state-space form, that is

$$\begin{aligned}
\dot{x}(t) &= Ax(t) + Bu(t) + Nw(t) & (4.1) \\
y(t) &= Cx(t) + Du(t) + v(t). & (4.2)
\end{aligned}$$

Here $y(t)$ represents the observation and $x(t)$ is the state vector of the system at the time t. The state propagation of the system in time, is described

by the state transition equation, Equation (4.1), and the measured signals by
the measurement equation, Equation (4.2). The noise terms $w(t)$ and $v(t)$
are assumed to be white stochastic processes and are referred to as process
noise and measurement noise respectively. They describe the imperfections
of the model. The covariance function and the mean value for the noise are
described by

$$E[w(t)] = E[v(t)] = 0 \tag{4.3}$$
$$E[w(t)w^T(\tau)] = Q_t\delta(t-\tau) \tag{4.4}$$
$$E[v(t)v^T(\tau)] = R_t\delta(t-\tau) \tag{4.5}$$
$$E[w(t)v^T(\tau)] = S_t\delta(t-\tau). \tag{4.6}$$

The stochastic variables could come from an arbitrary distribution, but in
the special case with normally distributed stochastic variables the resulting
Kalman filter is optimal. If this is the case equation (4.6) becomes

$$E[w(t)v^T(\tau)] = 0 \tag{4.7}$$

For simplicity, the following notation for the covariance matrix (without Dirac's
delta function) will be used in this thesis

$$\Pi = \begin{pmatrix} Q_w & S \\ S^T & R_v \end{pmatrix}. \tag{4.8}$$

Theorem 4.1 (Kalman estimator: Continuous time). *Consider the system
described by (4.1) and (4.2). Assume that A, C, Q_w, R_v and S fulfil the
following. R_v is symmetric and positively definite and $\tilde{Q}_w = Q_w - SR_v^{-1}S^T$
is positively semi definite. Assume that (A, C) is detectable and that $(A -
SR_v^{-1}C, \tilde{Q}_w)$ is possible to stabilize. Then the observer that minimizes the
prediction error*

$$\tilde{x}(t) = x(t) - \hat{x}(t) \tag{4.9}$$

is given by

$$\dot{\hat{x}} = A\hat{x} + Bu(t) + K(y(t) - C\hat{x}(t)) \tag{4.10}$$

where K is given by

$$K = (PC^T + NS)R_v^{-1}. \tag{4.11}$$

Here P is the symmetric positive semi definite solution of the matrix equation

$$AP + PA^T - KR_v^{-1}K^T + NQ_wN^T = 0 \tag{4.12}$$

and the variance of the minimal prediction error is given by

$$E[\tilde{x}(t)\tilde{x}^T] = P. \tag{4.13}$$

This is the Kalman observer. According to [FG01] the covariance matri-
ces represent the trust in the initial state and can therefore be seen as a design
variables.

For a more thorough description of the Kalman theory, consult e.g. [FG01],
[TG03] or [GM93].

4.1.2 Modelling and linearization errors

Figure 4.1 shows how the non-linear model is influenced by errors not only in the model derivation, but also in the linearization process. These errors are denoted Δ_1 and Δ_2, respectively. The Kalman filter may become impaired due to these errors.
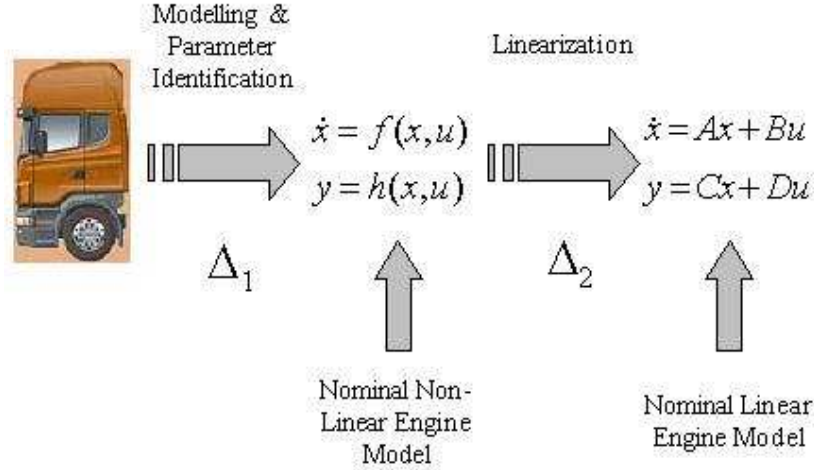
Figure 4.1: Modelling error representation.

If the presumed model uncertainties are part in the measurement and process noises, it means that these uncertainties are merged in the R, Q and S matrices. To put this into practice, the measurement noise and the process noise are given by

$$v = \tilde{y} \tag{4.14}$$
$$w = f_i(\hat{x}, u) - \dot{\tilde{x}}_i \tag{4.15}$$

where $\dot{\tilde{x}}$ is the derivative of the low pass filtered measured states and $\tilde{y}$ is the high-pass filtered measured signals. $\dot{\tilde{x}}$ is achieved by measuring all states, filter them with a non-causal filter and at last numerically differentiate them with an Euler backward method. $\tilde{y}$ consists of p_{im}, p_{em}, N_{trb}, W_{air} and T_{im}, which are the measured signals on a original engine in production. This filtering is made because all frequency components exceeding 2 Hz in the measured signals are considered to be measurement noise. The cut-off frequency of 2 Hz is chosen at this point since all system dynamics are slower than this. The low pass filtering of the measured signals in Equation 4.15 is necessary to remove the measurement noise and is performed before the differentiation. The covariance estimation in this thesis is performed in MATLAB with the

function `covf`. In the Equations (4.16) and (4.17) the algorithm is presented.

$$\hat{R}_{ij} = \frac{1}{N} \sum_{t=1}^{N} v_i(t)v_j(t) \qquad (4.16)$$

$$\hat{Q}_{ij} = \frac{1}{N} \sum_{t=1}^{N} w_i(t)w_j(t) \qquad (4.17)$$

These calculations of the R and Q matrices give the joint correlation between the signals in the measurement noise and system noise respectively.

When calculating the observer the relation between R and Q describes how strong the feedback from the measured signals is in the sensor fusion. To get satisfactory performance of the sensor fusion this relation is treated as a design parameter.

Calculation of covariance matrices for the noise

In this non-scalar model, the cross correlation between the measurement signals and the measured state signals will not be estimated for simplicity. This means that the Π matrix will become

$$\Pi = \begin{pmatrix} Q_w & 0 \\ 0 & R_v \end{pmatrix}. \qquad (4.18)$$

Due to the fact that the measured signals of the EGR system and the rest of the system are performed in two different measurement set-ups, the actual cross-correlation in the Q matrix is hard to calculate for those signals. The uncertainties in such estimation could be large, and therefore these correlations are not taken into account. This will give a Q matrix with the following properties

$$Q_w^{15\times15} = \begin{pmatrix} Q_{truck\ meas.}^{13\times13} & 0^{13\times2} \\ 0^{2\times13} & Q_{test\ bed\ meas.}^{2\times2} \end{pmatrix}. \qquad (4.19)$$

The $R_v^{5\times5}$ matrix does obviously not have these problems, and the calculation is straightforward with Equation (4.16).

4.2 Linearization

The system at hand is a typical non-linear system, and to be able to use the Kalman theory it has to be linearized. A non-linear time-continuous model

$$\dot{x} = f(x,u) + g(x,u)w_1 \qquad (4.20)$$
$$y = h(x,u) + w_2 \qquad (4.21)$$

can be linearized around a stationary point, $\dot{x} = f(x_0, u_0) = 0$. With the notation

$$z = x - x_0 \tag{4.22}$$
$$v = u - u_0 \tag{4.23}$$

and a Taylor series expansion, the linearized system will become

$$\dot{z} = Az + Bv \tag{4.24}$$
$$w = Cz + Dv. \tag{4.25}$$

Here the matrices A, B, C and D are the Jacobians of the functions $f(x, u)$ and $h(x, u)$ The elements $a_{ij}, b_{ij}, c_{ij}, d_{ij}$ in the matrices are given by

$$a_{ij} = \left.\frac{\partial f_i}{\partial x_j}\right|_{x=x_0, u=u_0} \tag{4.26}$$

$$b_{ij} = \left.\frac{\partial f_i}{\partial u_j}\right|_{x=x_0, u=u_0} \tag{4.27}$$

$$c_{ij} = \left.\frac{\partial h_i}{\partial x_j}\right|_{x=x_0, u=u_0} \tag{4.28}$$

$$d_{ij} = \left.\frac{\partial h_i}{\partial u_j}\right|_{x=x_0, u=u_0}. \tag{4.29}$$

4.2.1 Linearization procedure

The linearization process is a two step procedure. The first step is to find a stable operating point and the second is the linearization itself.

Finding a stationary operating point

The search for a stationary operating point is performed by simulating the model with constant inputs until stationary states are achieved. These inputs and states are used to define the operating point in which the linearization is performed.

Linearizing

The linearization procedure presented in Section 4.2 is performed by the function `linearize` in SIMULINK CONTROL DESIGN Toolbox. The function uses analytical Jacobians for all blocks possible. The non-linear blocks without analytical Jacobians, e.g. lookup tables, are replaced with gains when linearizing. The linearization results are presented in Section 7.1.

4.2.2   Scaling

When linearizing, it is important that the numerical properties of the received linearized system is good. Bad numerical properties can lead to instability and loss of precision. The standard way to improve system with bad numerical properties is to rescale the model states so that they are in the same order of magnitude, i.e. balanced realization. For example the numerical properties might improve if the pressure is modelled in bar instead of Pascal to get in the same order of magnitude as the temperature. This is not performed in this thesis because the linearized system does not show any tendencies of numerical problems.

4.2.3   Kalman filter and non-linear models

When using the Kalman theory on the non-linear model described by Equation (4.20) and (4.21), a number of different techniques can be used. Linearizing the model about the Kalman filter's estimated trajectory and then calculate a Kalman filter in this point in real time, is called the *extended Kalman filter*. This method is not feasible due to the model complexity which will make the linearization computationally demanding. Another way is to use the *constant gain extended Kalman filter (CGEKF)*. The CGEKF method linearizes the model in several operating points and calculates an observer for each linearization. The system then uses the observer nearest the current operating point and switches between these Kalman filters. The CGEKF is the approach in this thesis since all calculations can be made in advance and it is less computational demanding for the ECU on the engine.

According to [GM93] considerable non-linearities can sometimes lead to divergence for the CGEKF, or the *linearized Kalman filter* as they call it. The advice then is to use the extended Kalman filter. In this application however, this is not an option, and reducing the model might be necessary. In Chapter 7 the CGEKF does not show any tendencies to diverge, and the conclusion is that the non-linearities are not large enough to motivate model reduction. Note that this divergence depends on the operating point, how fast and large steps that are taken etc. This investigation covers normal operating points and steps.

Chapter 5

Measurement set-up

To be able to tune the parameters in the model and to validate the model, measurements are performed in order to collect data. The measurement set-up consists of a Scania R124 equipped with a new generation 470 hp six cylinder diesel engine with VGT and EGR. To make tuning of parameters and validation possible several extra temperature and pressure sensors are mounted in addition to the original ones.

Measurements carried out in the Scania vehicle are sampled and recorded with the measurement tool ATI Vision. This tool from Accurate Technologies Inc. allows access to the ECU:s (Electronic Control Unit) for, amongst other, calibration and logging measurement data.

5.1 Sensors

When tuning and validating the model parameters the original sensors on the test vehicle are not enough. The following sections present the sensors mounted in the vehicle. When tuning the parameters in the EGR system, data from a test bed are used. For a more thorough description of the sensors used, consult [Hol05].

5.1.1   Vehicle sensors

The sensors monted in the vehicle are listed in Table 5.1.

Sensor	Description
δ	Injected amount of fuel $[kg/s]$
n_{eng}	Engine speed $[rpm]$
n_{trb}	Turbine speed $[rpm]$
p_{im}	Pressure in the intake manifold $[bar]$
p_{em}	Pressure in the exhaust manifold $[bar]$
p_{amb}	Ambient pressure $[bar]$
p_{cmp}	Pressure after the compressor $[bar]$
p_{trb}	Pressure after the turbine $[bar]$
$p_{ExhBrake}$	Pressure after the exhaust brake $[bar]$
T_{im}	Temperature in the intake manifold $[^oC]$
T_{amb}	Ambient temperature $[^oC]$
T_{cmp}	Temperature after the compressor $[^oC]$
T_{trb}	Temperature after the turbine $[^oC]$
$T_{ExhBrake}$	Temperature after the exhaust brake $[^oC]$
T_{em}	Temperature in the exhaust manifold $[^oC]$
w_{air}	Air mass flow into the intake manifold $[kg/s]$

Table 5.1: Standard sensors.

5.1.2   Test bed sensors

The sensors monted in a test bed are listed in Table 5.2.

Sensor	Description
$p_{before,valve}$	Pressure before the EGR valve $[bar]$
$p_{after,valve}$	Pressure after the EGR valve $[bar]$
p_{EGR}	Pressure after the EGR air cooler $[bar]$
$T_{before,valve}$	Temperature before the EGR valve $[^oC]$
T_{EGR}	Temperature after the EGR air cooler$[^oC]$

Table 5.2: Test bed sensors.

Chapter 6

Parameter estimation

In this chapter the parameter estimation will be presented. The normal way to estimate a parameter is to split the data sequence in two parts, one for modelling and one for validation. This is also the routine in this thesis. The parameter estimation is performed with the least-square method on the measured data. Considered errors are

$$\text{Mean relative error} \quad = \quad \frac{1}{N} \sum_{i=1}^{N} \frac{|\hat{x}(t_i) - x(t_i)|}{|\hat{x}(t_i)|} \tag{6.1}$$

$$\text{Maximum relative error} \quad = \quad \max_{1 \leq i \leq N} \frac{|\hat{x}(t_i) - x(t_i)|}{|\hat{x}(t_i)|}. \tag{6.2}$$

6.1 Intercooler heat exchanger efficiency

In Section 3.3.3 a heat exchanger model with constant efficiency is presented. This parameter is estimated with data from the Scania truck presented in Section 5. The result is presented in Table 6.1 and the estimation errors are listed in Table 6.2. The performance for the model of the heat exchanger efficiency in the Intercooler can be seen in Figure 6.1.

Parameter	Value
ϵ_{ic}	83.6 %

Table 6.1: The parameter for the heat exchanger efficiency in the Intercooler.

Parameter	Mean relative error	Max relative error
ϵ_{ic}	1.3 %	6.4 %

Table 6.2: The relative mean and maximum errors in the Intercooler efficiency estimation.
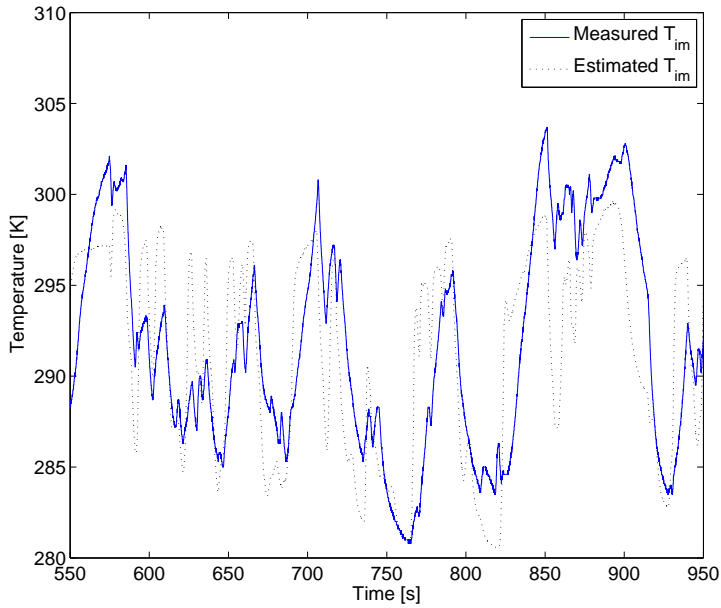
Figure 6.1: Intercooler efficiency.

According to Figure 6.1 the model over the heat exchanger efficiency is quite good. It is hard to model a simple efficiency model for heat exchangers in trucks where for example vehicle speed, wind speed and other unknown disturbance sources influences the efficiency.

6.2   EGR cooler

The EGR cooler consist, as mentioned in Section 3.9, of a heat exchanger and a restriction. The parameters describing these models are estimated with data from an engine in a test bed at Scania.

6.2.1 EGR mass flow

To estimate the restriction model the EGR mass flow is needed. There is no sensor for this mass flow and it is therefore calculated with Equation (6.3).

$$W_{egr} = \eta_{vol} \frac{p_{im} V_D N_{cyl} N}{T_{im} R \cdot 2 \cdot 60} - W_{air} \tag{6.3}$$

Here is η_{vol} the volumetric efficiency, V_D the displacement volume and N_{cyl} the number of cylinders of the engine.

6.2.2 EGR cooler efficiency

In Section 3.9.2 a model with constant efficiency is proposed. The result is listed in Table 6.3 and the estimation errors are listed in Table 6.4.

Parameter	Value
ϵ_{egr}	76.8 %

Table 6.3: The parameter for the efficiency model in the EGR cooler.

Parameter	Mean relative error	Max relative error
ϵ_{egr}	9.1 %	35.7 %

Table 6.4: The relative mean and maximum errors in the EGR cooler efficiency estimation.

The maximum relative error is considerable and an explanation for this is that the model is simple. The EGR cooler is over dimensioned and manages to lower the gas temperature to just a few degrees over the temperature of the cooled supercharged air. This makes it hard to model. Other physical parameters affecting the EGR cooler efficiency could e.g. be the EGR flow and the temperature of the EGR gas. One should also remember that this test was performed in a test bed, and the efficiency in a truck will vary even more because of differences in the cooling air mass flow. Some measurements indicate efficiency higher than one. This means the exhaust gas is cooled to a lower temperature than the cooling air, which is physically impossible. An explanation for this could e.g. be a bad location for the temperature sensors for certain flows, or cooling of the temperature sensor due to condensed air in the exhaust gas. Read more about validation of temperature sensor values by Ericson in [Eri04].

6.2.3   EGR cooler restriction

The EGR cooler restriction contains one tuning parameter, H_{res} and the result can be seen in Table 6.5. The estimation errors are listed below in Table 6.6.

Parameter	Value
H_{res}	$5.1849 \cdot 10^6$

Table 6.5: The parameter in the EGR cooler restriction.

Parameter	Mean relative error	Max relative error
H_{res}	$5.0\,\%$	$55.6\,\%$

Table 6.6: The relative mean and maximum errors in the EGR cooler restriction estimation.

The performance for the model of the EGR cooler restriction can be seen in Figure 6.2.
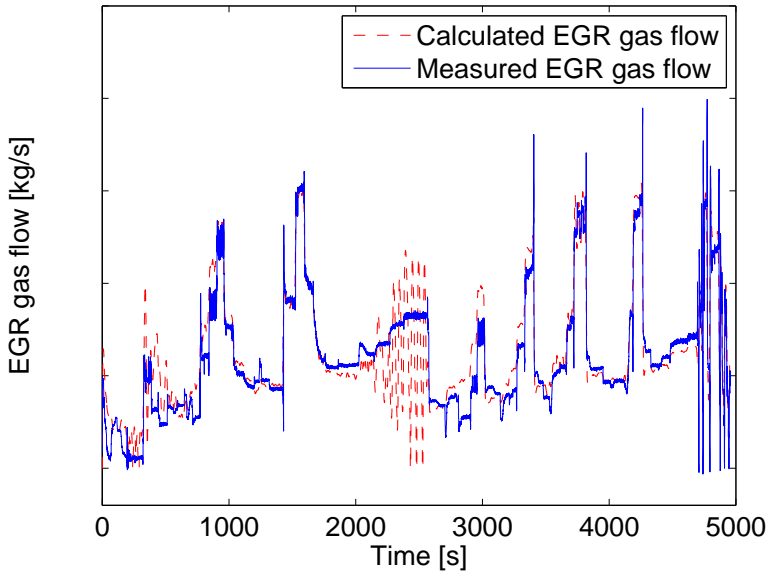
Figure 6.2: EGR cooler restriction.

According to this figure the model for the EGR cooler restriction describes the flow through the cooler very good.

6.3   Heat transfer in the exhaust manifold

The parameters estimated in the heat transfer model in Section 3.6.1, are the parameter $T_{amb,corr}$ and the lumped parameter $h_{tot}A$. These parameters are estimated with data from a Scania truck. $T_{amb,corr}$ is manually adjusted to minimize the estimation errors of $h_{tot}A$. The parameters are listed in Table 6.7. The estimation errors related to $h_{tot}A$ are listed in Table 6.8.

Parameter	Value
$h_{tot}A$	$195\,J/Ks$
$T_{amb,corr}$	$180K$

Table 6.7: The parameters in the heat transfer model.

Parameter	Mean relative error	Max relative error
$h_{tot}A$	$21.1\,\%$	$62.4\,\%$

Table 6.8: The relative mean and maximum errors in the heat transfer parameter estimation.

The performance for the model of the heat transfer in the exhaust manifold can be seen in Figure 6.3. According to this figure the model of the heat transfer in the exhaust manifold improves the exhaust gas temperature model with approximately 50 %. This means that even though the value for $h_{tot}A$ are inaccurate according to Table 6.8, the estimation for exhaust gas temperature is improved.
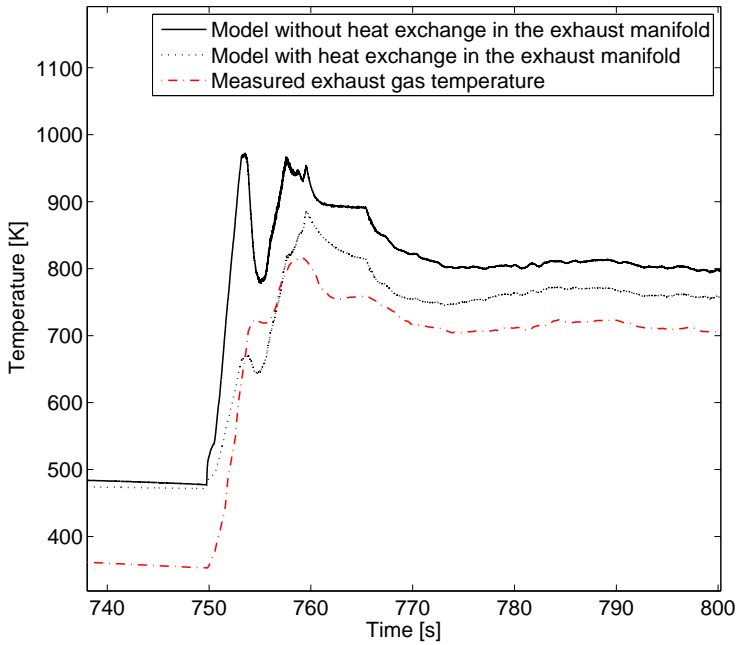
Figure 6.3: Heat transfer in the exhaust manifold.

Chapter 7

Results

This chapter presents the results of the modelling, linearization and the Kalman feedback. The results are obtained by simulating the model presented in Chapter 3 and the linearized model in Section 4.2, using the estimated parameters from Chapter 6, with data from a Scania truck.

7.1 Linearization

In this section the result from the linearization procedure in Section 4.2 is presented. All three models are linearized but only the result of the fully extended is presented.

Step responses from all inputs are simulated for both the linear and the non-linear model. The steps in the inputs are made after 10 seconds. To enlighten the non-linear effects in the model, the magnitudes of the steps are 20 % and 1 % of respective input. A comparison shows that the correspondence, i.e. the time constants and the gains, between the linear and the non-linear model are good for small steps but not so good for larger steps. Some of the step responses are presented below together with short comments. All these step responses originate from the same stationary operating point, but the non-linear effects can vary between different operating points. This cannot be seen here.

Step in u_{egr} to output W_{air}

Increasing u_{egr} corresponds to opening the EGR valve which results in an increase in the EGR mass flow, W_{egr}. This means that the air mass flow, W_{air}, decreases. This phenomena and the non-linear effects can be seen in Figure 7.1 and Figure 7.2.
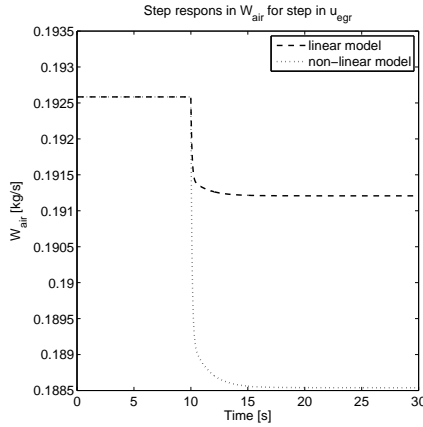
Figure 7.1: Step respons in W_{air} for the linear and the non-linear model with a 20 % step in u_{egr}.
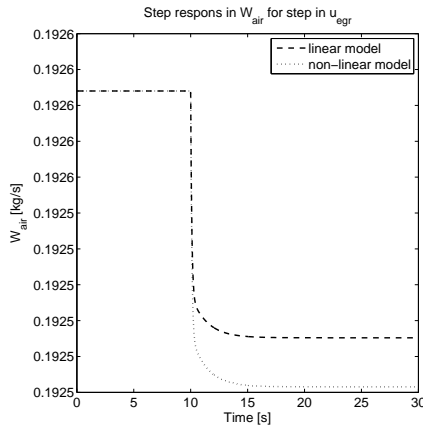
Figure 7.2: Step respons in W_{air} for the linear and the non-linear model with a 1 % step in u_{egr}.

Step in u_{vgt} to output p_{im}

Increasing u_{vgt} corresponds to decreasing the effective flow area in the turbine which results in a higher gas velocity. This implies that the turbine speed increases and the compressor will therefore increase the pressure in the inlet manifold, p_{im}. This phenomena and the non-linear effects can be seen in Figure 7.3 and Figure 7.4.
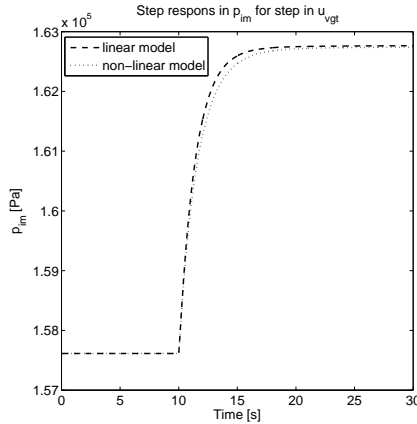
Figure 7.3: Step respons in p_{im} for the linear and the non-linear model with a 20 % step in u_{vgt}.
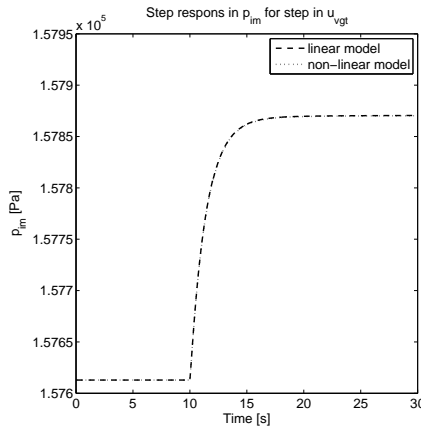
Figure 7.4: Step respons in p_{im} for the linear and the non-linear model with a 1 % step in u_{vgt}.

Step in u_{egr} to output p_{im}

As stated above, increasing u_{egr} corresponds to opening the EGR valve which results in an immediate increase of the EGR mass flow, W_{egr}. This in turn results in an immediate increase in the inlet manifold pressure, p_{im}. However, opening u_{egr} also means that more exhaust gases are recirculated and less exhaust gases are left to drive the turbine. This causes the turbine to slow down which results in a larger decrease in p_{im} than the initial increase. These phenomena and the non-linear effects can be seen in Figure 7.5 and Figure 7.6.
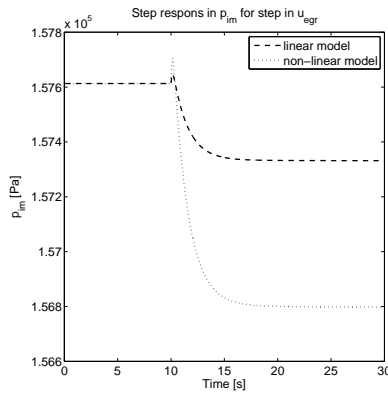
Figure 7.5: Step respons in p_{im} for the linear and the non-linear model with a 20 % step in u_{egr}.
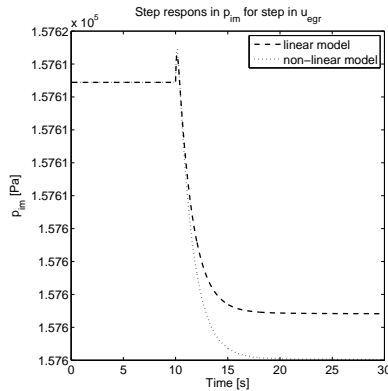
Figure 7.6: Step respons in p_{im} for the linear and the non-linear model with a 1 % step in u_{egr}.

Step in u_{vgt} to output W_{air}

As stated above, increasing u_{vgt} corresponds to a decrease of the effective flow area in the turbine such that the exhaust gas flow through it is more restricted. If the EGR valve is sufficiently open when this happens, the exhaust gas recirculation, W_{egr}, will increase and W_{air} will decrease. On the other hand, if the EGR valve is closed when the exhaust gas flow through the turbine is restricted, W_{egr} cannot increase and the effect will be that the turbine speed increases and W_{air} will increase. The latter phenomena and the non-linear effects can be seen in Figure 7.7 and Figure 7.8.
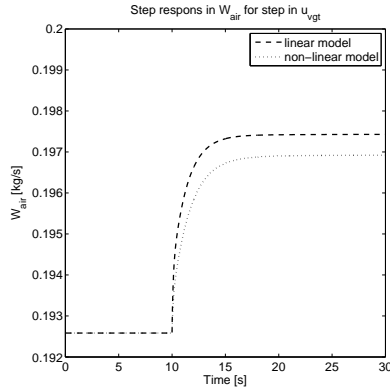
Figure 7.7: Step respons in W_{air} for the linear and the non-linear model with a 20 % step in u_{vgt}.
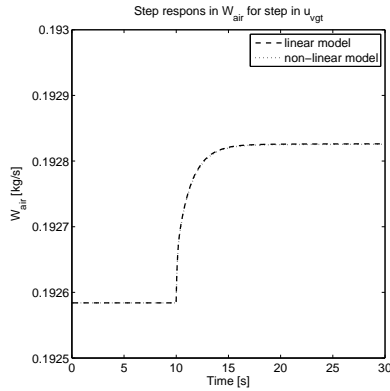
Figure 7.8: Step respons in W_{air} for the linear and the non-linear model with a 1 % step in u_{vgt}.

7.2   Model comparison

In this section three models with different complexity are compared. The models are:

- The model presented by Swartling in [Swa05], sometimes referred to as the original model.

- The model above extended with a state for the temperature in the intake manifold.

- The fully extended model with states for all temperatures.

A plot of the models for p_{im} and the measured signal for p_{im} is given in Figure 7.9. The reason for choosing p_{im} as the signal measuring the performance is that this signal is important in the calculation of the λ-value.

As seen in Figure 7.9, the best correspondence with the measured signal is achieved by the fully extended model followed by the original model without a state for the temperature in the intake manifold. However, the reason for extending the model with a model for the intake manifold temperature is to be able to use the signal for feedback and, by that, improve the observer.

In Table 7.1 the mean relative error and maximum relative error for the three different models are listed. These figures verify that the best model is the fully extended model.

Model	Mean rel. error	Max rel. error
Extended model, states for all temp.	4.55 %	16.8 %
Swartling's model with state for T_{im}	13.2 %	24.8 %
Swartling's model	11.9 %	21.7 %

Table 7.1: The mean relative error and the maximum relative error for the three models.

7.3   Kalman feedback

The models in Section 7.2 are linearized, and upon this an observer is calculated. To handle the non-linearities in the model the linearized Kalman filter is used, see Section 4.2.3.

To find the best relation between the number of Kalman filters and the model complexity, three sets of models and three sets of Kalman filters are compared to find the best total performance. These comparisons are made in two steps. Section 7.3.1 discusses the number of Kalman filters used for feedback and Section 7.3.2 treats the model complexity.
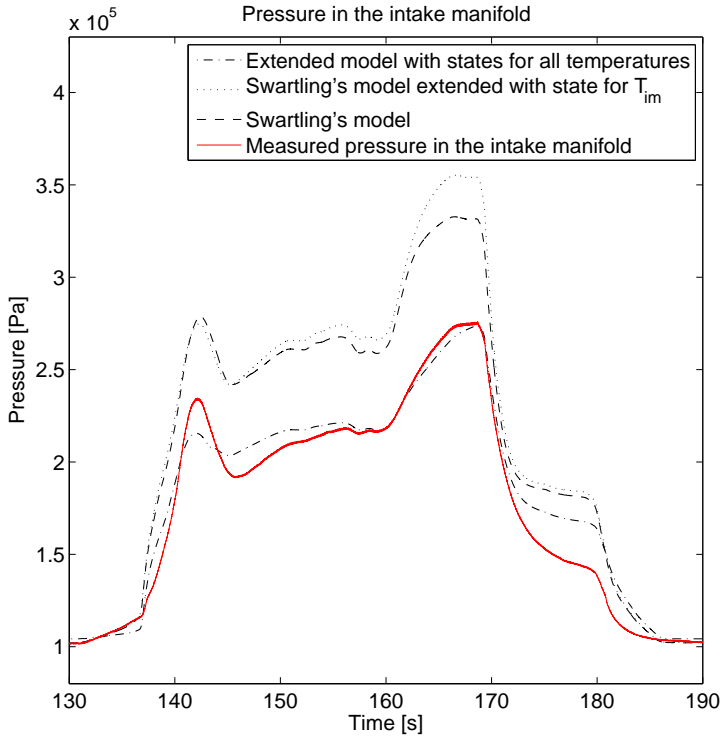
Figure 7.9: Comparison of p_{im} for all three models.

7.3.1 Number of linearization points

When the model is simulated with the Kalman feedback, one has to choose the number of Kalman filters used in the observer. In [Swa05] the number of Kalman filters is estimated to be around ten for the best performance. Three observers with different number of Kalman filters are tested in the fully extended model. The numbers of Kalman filters tested in the observers are 3, 9 and 16. Figure 7.10 shows that it is difficult to distinguish the best observer. The performances of the observers are also compared using the mean relative error and the maximum relative error in Table 7.2. This table indicates that the observer with 9 Kalman filter has the best overall performance.
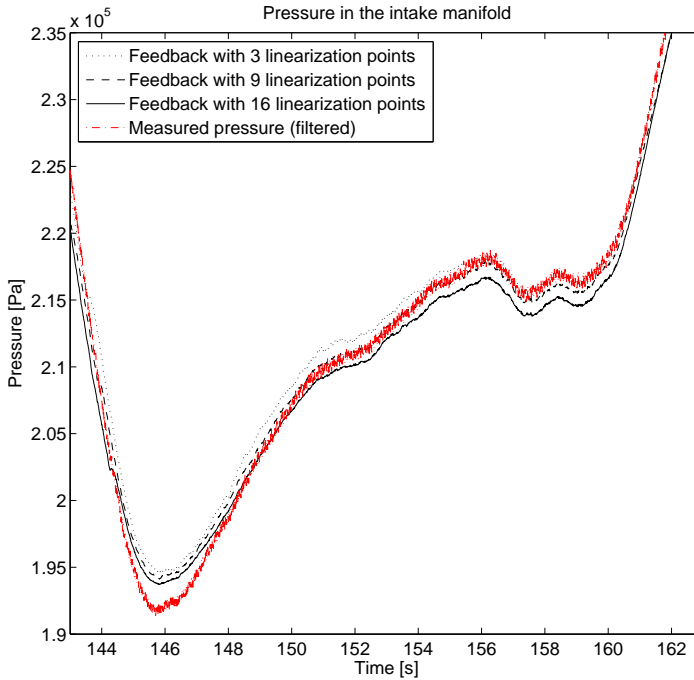
Figure 7.10: The difference between the models with Kalman feedback seems to be negligible. Despite the conformity an error estimation shows some differences.

Number of linearization points	Mean rel. error	Max rel. error
3 linearization points	1.52 %	7.51 %
9 linearization points	1.10 %	5.60 %
16 linearization points	1.70 %	5.96 %

Table 7.2: The mean relative error and the maximum relative error for the three different sets of linearization points in the observer.

The pressure in the exhaust manifold is difficult to estimate accurately. This can be seen in Figure 7.11. The reason for the difference between the model and the measured signal in the fast and the slow transient for p_{em} is that the model has too slow dynamics. The fast transient is to the left and the slow is to the right in Figure 7.11.

The performance for the observer in the estimation of p_{em} is expressed in terms of the mean relative error and the maximum relative error as above. The errors are listed in Table 7.3.
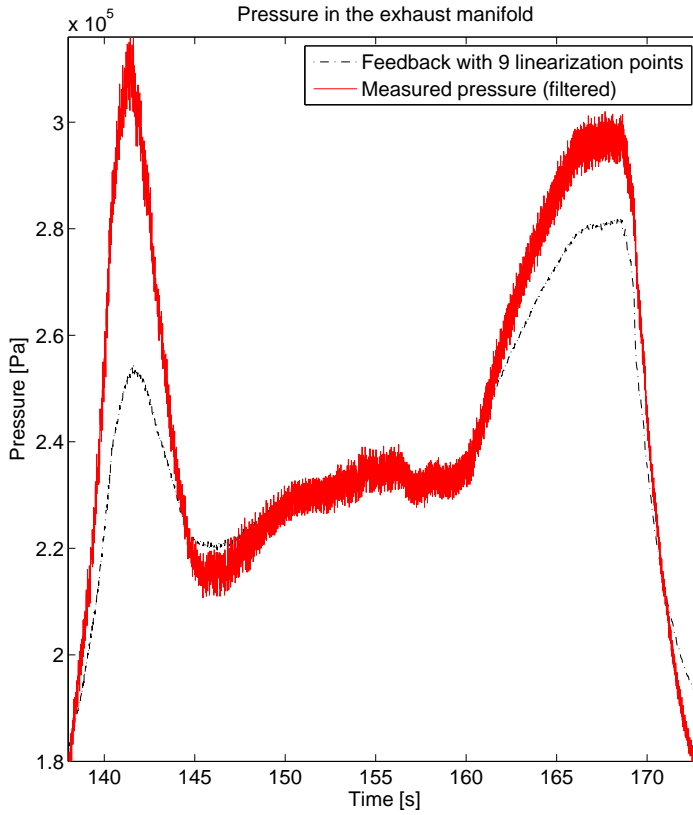
Figure 7.11: The estimation of p_{em} is not good.

Number of linearization points	Mean rel. error	Max rel. error
9 linearization points	7.13 %	26.0 %

Table 7.3: The mean relative error and the maximum relative error for the set of nine linearization points in the estimation of p_{em}.

7.3.2 Model complexity

The observers used in this comparison use 9 linearization points, which is considered to give the best performance. The result can be viewed in Figure 7.12. The figure shows that a more complex model gives a better estimation of the pressure in the intake manifold.

The performances of the observers for the different models are also com-
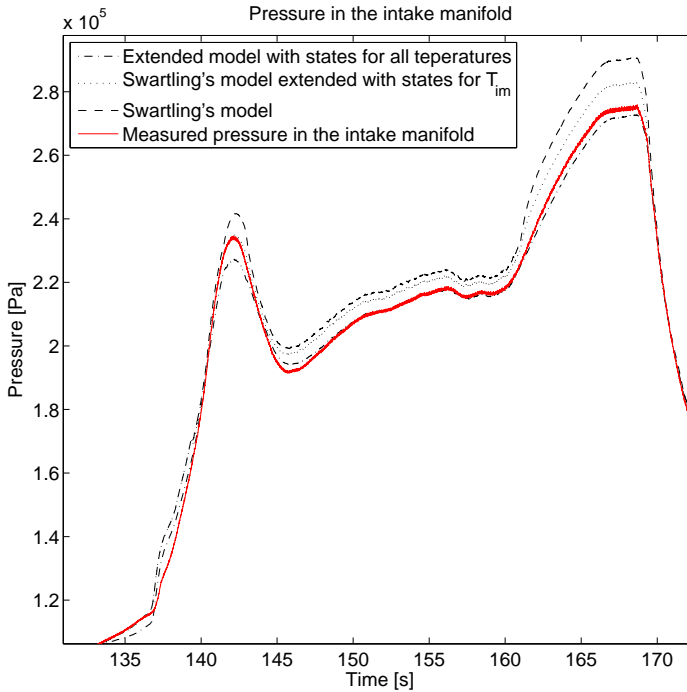
Figure 7.12: The figure shows that the best model when using 9 linearization points is the extended model, with states for all temperatures. Swartling's model with and without a state for T_{im} has almost equal performance.

pared using the mean relative error and the maximum relative error. The errors are listed in Table 7.4. The extended model is obviously better according to the error estimation as well.

Model	Mean rel. error	Max rel. error
Extended model, states for all temp.	1.10 %	5.60 %
Swartling's model with states for T_{im}	2.07 %	3.78 %
Swartling's model	3.55 %	6.24 %

Table 7.4: The extended model has better performance in both mean relative error and maximum relative error.

Chapter 8

Concluding remarks

This chapter contains the conclusions together with a short summary of the obtained results and observations made. It also includes a section in which interesting future work is introduced.

8.1 Conclusions and discussion

The goal of this thesis is to improve the gas flow observer introduced in [Swa05]. The evaluation is performed on several data sets from a Scania truck.

The noise in the air mass flow sensor is examined and characterized in the frequency domain. The result of this investigation shows that the approach presented in this thesis does not apply to the noise in the air mass flow sensor and another approach is needed.

Kalman theory is used to calculate the observer and this requires a linear model. The models in this thesis are non-linear and the linearizations are performed with SIMULINK CONTROL DESIGN with good results.

The original model has been extended in two stages to include more system dynamics. In the first stage a temperature state in the intake manifold is introduced. In the second stage the model is extended with temperature states for all control volumes and with complete dynamics for the EGR system and the exhaust system including the exhaust brake. These models are compared in how good they coincide with the measured signals. The comparison shows that the best model is the fully extended model followed by the first stage extended model.

8.2 Future work

In this thesis the mixing of EGR gas and supercharged air takes place before the intake manifold. A more realistic model would be to model the mixing of

these gases after the control volume, right before the engine.

The choice of a static model for the heat transfer in the exhaust manifold can be motivated by the fact that the existing model already catches the dynamics well but models the temperature of the exhaust gases too high. Nevertheless, here are some possibilities of future work. A first suggestion would be to model the wall temperature with the dynamic model presented by Eriksson in [Eri02].

The extended model presented in this thesis can be improved by tuning some of the control volumes better. The control volumes not properly tuned are those present in the original model, which are tuned for a model not containing dynamics for the temperatures.

Simulations show that the model of the pressure after the combustion, i.e. the pressure in the outlet manifold, is not so good. Hence, this is a suggestion for some future work.

Since the engine has VGT the choice of using the signal from the turbine speed to choose filter in the observer is not so good. For a conventional turbo this choice is good since the speed of the turbo has a fairly simple relation to the load of the engine. This is not the case when a VGT is used. Therefore a thorough investigation of which signals to choose filter with, is necessary.

One way to improve the performance of the observer is to model the noise in the air mass flow sensor in a different way to achieve a better feedback signal.

References

[And05] P. Andersson. *Air Charge Estimation in Turbocharged Spark Ignition Engines*. Phd thesis 989, Department of Electrical Engineering, Linköpings Universitet, Linköping, Sweden, November 2005.

[Elf02] D. Elfvik. Modelling of a diesel engine with vgt for control simulations. Master's thesis IR-RT-EX-0216, Department of Signals, Sensors and Systems, Royal Institute of Technology, Stockholm, Sweden, July 2002.

[Eri02] L. Eriksson. Mean value models for exhaust system temperatures. SAE Technical Paper Series 2002-01-0374, Vehicular Systems, Linköpings Universitet, Linköping, Sweden, 2002.

[Eri04] C. Ericson. Mean value modelling of a poppet valve egr-system. Master's thesis LiTH-ISY-EX-3543-2004, Department of Electrical Engineering, Linköping University, Linköping, Sweden, June 2004.

[FG01] M. Millnert F. Gustafsson, L. Ljung. *Signalbehandling*. Studentlitteratur, Studentlitteratur, Lund, 2 edition, 2001.

[GM93] J. Minkler G. Minkler. *Theory and Application of Kalman Filtering*. Magellan Book Company, Palm Bay, FL, 1993.

[Hol05] A. Holmgren. Mean value modelling of the intake manifold temperature. Master's thesis LiTH-ISY-EX-3648-2005, Department of Electrical Engineering, Linköping University, Linköping, Sweden, June 2005.

[Lju99] L. Ljung. *System Identification - Theory for the user*. Prentice-Hall, Inc, Upper Saddle River, New Jersey 07458, 2 edition, 1999.

[LN04] L. Eriksson L. Nielsen. *Course material, Vehicular Systems*. Department of Electrical Engineering, Linköping University, 2004.

[OF03] M. Gustafsson O. Flärdh. Mean value modelling of a diesel engine with turbo compound. Master's thesis LiTH-ISY-EX-3443-2003, Department of Electrical Engineering, Linköping University, Linköping, Sweden, December 2003.

[Rit03] J. Ritzén. Modelling and fixed step simulation of a turbo charged diesel engine. Master's thesis LiTH-ISY-EX-3442-2003, Department of Electrical Engineering, Linköping University, Linköping, Sweden, June 2003.

[Swa05] F. Swartling. Gas flow observer for diesel engines with egr. Master's thesis LiTH-ISY-EX-3692-2005, Department of Electrical Engineering, Linköping University, Linköping, Sweden, June 2005.

[TG03] L. Ljung T. Glad. *Reglerteori - Flervariabla och olinjära system*. Studentlitteratur, Studentlitteratur, Lund, 2 edition, 2003.

Notation

Symbols used in the report.

Variables and parameters in chapter 2

I	Noise intensity/variance
$m(t)$	Time dependent mean value
m_t	Time independent mean value
n_{trb}	Turbine/Compressor speed
$r(t_1, t_2)$	Auto-correlation function

Variables and parameters in Chapter 3

A	Area
c_p	Specific heat at constant pressure
c_v	Specific heat at constant volume
ϵ	Efficiency, $0 \le \epsilon \le 1$
h	Heat transfer coefficient
H	Flow restriction coefficient
$\dot{H}$	Enthalphy flow
m	Mass
$\dot{m}$	Mass flow
p	Pressure
$\dot{Q}$	Heat transfer
R	Ideal gas constant
T	Temperature
U	Internal energy
V	Volume
W	Mass flow

Variables and parameters in Chapter 4

$\delta(t - \tau)$	Dirac's delta function
$E[\cdot]$	Expectation value

Variables and parameters in Chapter 6

η_{vol}	Volumetric efficiency
N_{cyl}	Number of cylinders
V_D	Displacement volume

Indices

amb	Ambient
cmp	Compressor
$cool$	Cooling
cv, i	Convection, Internal
cv, e	Convection, Engine block
cd, e	Conduction, Engine block
ds	Down stream
eff	Effective
egr	EGR air cooler
em	Exhaust manifold
es	Exhaust system
eng	Engine
exh	Exhaust
ic	Intercooler
im	Inlet manifold
lin	Linearization
rad	Radiation
res	Restriction
t	Time dependent
tot	Total
trb	Turbine
us	Up stream
vgt	Variable geometry turbine

Acronyms

$CGEKF$	Constant gain extended Kalman filter
ECU	Electronic control unit
EGR	Exhaust gas recirculation
ETC	European transient cycle
$MVEM$	Mean value engine model
VGT	Variable geometry turbine

Copyright

Svenska

Detta dokument hålls tillgängligt på Internet - eller dess framtida ersättare - under en längre tid från publiceringsdatum under förutsättning att inga extra-ordinära omständigheter uppstår.

Tillgång till dokumentet innebär tillstånd för var och en att läsa, ladda ner, skriva ut enstaka kopior för enskilt bruk och att använda det oförändrat för ickekommersiell forskning och för undervisning. Överföring av upphovsrätten vid en senare tidpunkt kan inte upphäva detta tillstånd. All annan användning av dokumentet kräver upphovsmannens medgivande. För att garantera äktheten, säkerheten och tillgängligheten finns det lösningar av teknisk och administrativ art.

Upphovsmannens ideella rätt innefattar rätt att bli nämnd som upphovsman i den omfattning som god sed kräver vid användning av dokumentet på ovan beskrivna sätt samt skydd mot att dokumentet ändras eller presenteras i sådan form eller i sådant sammanhang som är kränkande för upphovsmannens litterära eller konstnärliga anseende eller egenart.

För ytterligare information om Linköping University Electronic Press se förlagets hemsida: `http://www.ep.liu.se/`

English

The publishers will keep this document online on the Internet - or its possible replacement - for a considerable time from the date of publication barring exceptional circumstances.

The online availability of the document implies a permanent permission for anyone to read, to download, to print out single copies for your own use and to use it unchanged for any non-commercial research and educational purpose. Subsequent transfers of copyright cannot revoke this permission. All other uses of the document are conditional on the consent of the copyright owner. The publisher has taken technical and administrative measures to assure authenticity, security and accessibility.

According to intellectual property law the author has the right to be mentioned when his/her work is accessed as described above and to be protected against infringement.

For additional information about the Linköping University Electronic Press and its procedures for publication and for assurance of document integrity, please refer to its WWW home page: `http://www.ep.liu.se/`